Volume 9 | Number 19 | 7 October 2025

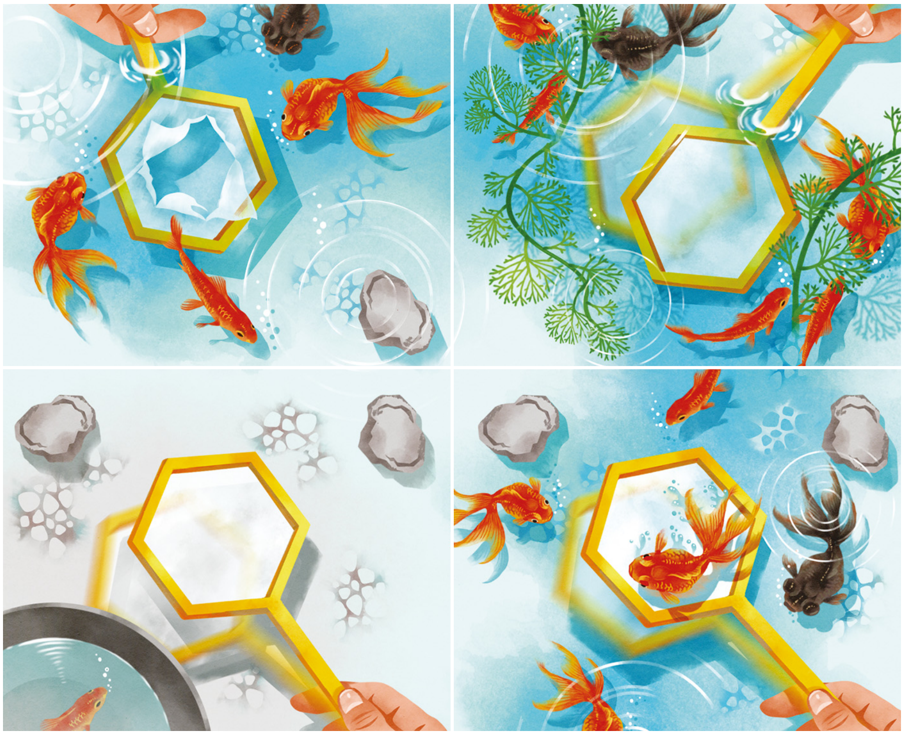

MATERIALS CHEMISTRY FRONTIERS

CCS 中国化学会 CHINESE CHEMICAL SOCIETY
ICCAS
ROYAL SOCIETY OF CHEMISTRY
rsc.li/frontiers-materials

MATERIALS CHEMISTRY FRONTIERS

RESEARCH ARTICLE

View Article Online
View Journal | View Issue

Check for updates

Cite this: *Mater. Chem. Front.*, 2025, **9**, 2863

A redox reaction triggered by hydrostatic pressure in dicationic cyclophanes†

Moto Kikuchi,[a] Tomoya Kuwabara,[b] Gaku Fukuhara, *[bc] Takanori Suzuki [a] and Yusuke Ishigaki *[a]

Received 16th June 2025, Accepted 14th July 2025

DOI: 10.1039/d5qm00426h

rsc.li/frontiers-materials

Various reactions and systems that respond to hydrostatic pressure, *i.e.*, one type of mechanical isotropic stimulus, have been developed over the past decades. Here, we show that a one-electron (1e) reduction of dicationic cyclophane can be realised by applying hydrostatic pressure in a water-containing solvent. The large negative value of the volume change $\left(\Delta V_T^{\circ}\right)$ observed for this reduction, which is key to inducing the reduction reaction, is due to the desolvation of the H_2O molecules and the change in the proximity between the cyclophane π units accompanied by a decrease in electrostatic repulsion. In fact, related monocations did not undergo a 1e reduction under hydrostatic pressure, even in water-containing solvents, indicating that the reduction behaviour is enabled by the cyclophane structure. Furthermore, in the case of weakly polar anions such as BF_4^- and PF_6^-, a change in the solvation/desolvation of the H_2O molecules of dicationic cyclophanes can occur upon hydrostatic pressurisation, leading to a 1e reduction, showing that the reduction behaviour can be tuned by selecting the appropriate counter anion. Therefore, this study provides a valuable strategy and guidelines for the rational design of molecules with redox behaviour that can be modulated using hydrostatic pressure.

Introduction

Stimuli-responsive materials have attracted wide interest in a variety of fields, such as supramolecular polymers, nanoparticles, and organic light-emitting diodes, because they can modulate various properties in response to external stimuli such as mechanical force, heat, light, and electric potential.[1–4] Hydrostatic pressure, one type of mechanical isotropic stimulus, has been investigated since the early 1960s.[5–7] Given that hydrostatic pressurisation of a solution can control the thermodynamic equilibrium and reaction kinetics,[7–9] various reactions in solution under an applied hydrostatic pressure have been investigated. For example, hydrostatic pressure has been shown to disturb the equilibrium of a reaction so that it behaves differently compared to at ambient pressure,[10–18] and thus some reactions are drastically accelerated under high pressure.[19,20] Recently, unique behaviour and systems, such as the dynamic control of chiral recognition induced by hydrostatic pressure[21] and ratiometric chemosensors that are capable of quantifying the degree of hydrostatic pressure,[22] have been reported. Therefore, the study of the effects of hydrostatic pressure has regained significant attention.[23]

$$-RT\ln K = \Delta G$$

$$\Delta G = \Delta H - T\Delta S \quad (1)$$

$$\Delta G = \Delta F + P\Delta V \quad (2)$$

When analysing chemical reactions or equilibria in solution, eqn (1) and (2) (where R is the gas constant, T is the temperature, K is the equilibrium constant, ΔF is the change in the Helmholtz energy, ΔV is the change in the volume, and ΔG is the change in the Gibbs energy) are typically used and the reaction proceeds spontaneously when ΔG is negative. Under conditions of constant pressure, *e.g.*, atmospheric pressure, ΔG is determined by two mutually correlated parameters,[24] *i.e.*, the changes in the enthalpy (ΔH) and the entropy (ΔS) (eqn (1)). The ΔS term is mainly affected by the solvation, but it is difficult to predict due to the vast number of solvating molecules in the solution. Therefore, it is not easy to predict the values of ΔH and ΔS to design a system with a negative ΔG term. On the other hand, under conditions of constant temperature, the ΔG term is determined by two different

[a] *Department of Chemistry, Faculty of Science, Hokkaido University, Sapporo 060-0810, Japan. E-mail: yishigaki@sci.hokudai.ac.jp*

[b] *Department of Chemistry, Institute of Science Tokyo, Meguro-ku, Tokyo 152-8551, Japan*

[c] *Institute for Materials Chemistry and Engineering, Kyushu University, Fukuoka 819-0395, Japan. E-mail: gaku@ms.ifoc.kyushu-u.ac.jp*

† Electronic supplementary information (ESI) available: Photographs for experimental apparatus; Experimental sections; hydrostatic pressure spectroscopic results; DFT calculations. CCDC 2446622. For ESI and crystallographic data in CIF or other electronic format see DOI: https://doi.org/10.1039/d5qm00426h

parameters, *i.e.*, ΔF and ΔV. If the pressure (P) is sufficiently large and the ΔV term is negative, the ΔG term would be negative. Compared to the ΔS term, the ΔV term is more predictable because it is based on a change in the structure and the solvation/desolvation process (eqn (2)). A change in the van der Waals volume during the reaction also contributes to the ΔV term, eventually enabling us to exert dynamic control of a targeted solution-state system through the application of pressure.

Cyclophanes that can exhibit flexible change in conformation have attracted considerable attention due to their ability to modulate physical properties through the inclusion and exclusion of guest molecules.[25–32] As these processes are accompanied by changes in the van der Waals volume, their potential responsiveness to hydrostatic pressure is of particular interest. In addition, there have been pioneering studies[33–36] on cationic cyclophanes, such as Stoddart's "blue box," the properties of which can also be controlled by an electric potential.[37–39] However, the effect of hydrostatic pressure on physical properties as well as redox behaviour remains elusive. Only a few studies on pressure-controlled redox reactions have been reported so far,[40] probably due to the small change in the van der Waals volume upon electron transfer in reversible organic redox systems. Here, we envisaged that cyclophane-type dication $\mathbf{2}^{2+}$,[41] which should undergo a large change in molecular structure that depends on its redox state, could be a suitable candidate to study how pressure affects a redox reaction. This is because the change in the apparent reaction volume at a certain constant temperature of T $\left(\Delta V_T^{\circ}\right)$ can be expected to change upon electron transfer. The ΔV_T° term for $\mathbf{2}^{2+}$ can be expressed as shown in eqn (3) and (4).

$$\Delta V_T^{\circ} = \left(V_{\mathbf{2}^{\bullet+}}^{\circ} + V_{\mathbf{2}^{\bullet+},\mathrm{sol}}^{\circ}\right) - \left(V_{\mathbf{2}^{2+}}^{\circ} + V_{\mathbf{2}^{2+},\mathrm{sol}}^{\circ}\right) \tag{3}$$

$$\Delta V_T^{\circ} = \left(V_{\mathbf{2}^{\bullet+}}^{\circ} - V_{\mathbf{2}^{2+}}^{\circ}\right) + \left(V_{\mathbf{2}^{\bullet+},\mathrm{sol}}^{\circ} - V_{\mathbf{2}^{2+},\mathrm{sol}}^{\circ}\right) \tag{4}$$

Here, the subscripts $\mathbf{2}^{\bullet+}$ and $\mathbf{2}^{2+}$ represent the van der Waals volume of the radical cation and dication, while $\mathbf{2}^{\bullet+}$, sol and $\mathbf{2}^{2+}$, sol refer to the solvated molar volume of the radical cation and dication, respectively. Given that dication $\mathbf{2}^{2+}$ contains two xanthylium units linked by flexible alkylene spacers, both the distance between the tricyclic π skeletons and the overall molecular conformation can change dynamically in solution, something which cannot be realised by reference monocation $\mathbf{1}^{+}$ with a monomeric structure (Fig. 1).[41] During a one-electron (1e) reduction of $\mathbf{2}^{2+}$, the electrostatic repulsion between the tricyclic π skeletons can be expected to be reduced so that the stacking distance between the π units would decrease. In other words, the $\left(V_{\mathbf{2}^{\bullet+}}^{\circ} - V_{\mathbf{2}^{2+}}^{\circ}\right)$ term in eqn (4) can be expected to be negative for the reduction of $\mathbf{2}^{2+}$. In addition, the $\left(V_{\mathbf{2}^{\bullet+},\mathrm{sol}}^{\circ} - V_{\mathbf{2}^{2+},\mathrm{sol}}^{\circ}\right)$ term in eqn (4) can be expected to be negative due to desolvation caused by the smaller charge on the radical cation. Thus, the ΔV_T° value should be negative and the 1e reduction of $\mathbf{2}^{2+}$ is expected to be facilitated when hydrostatic pressure is applied. Here, we report a serendipitous discovery that cyclophane-type dication $\mathbf{2}^{2+}$ can be easily reduced in a water-containing solvent by applying hydrostatic pressure. We also reveal that the reduction behaviour changes for different salts of the same dicationic cyclophane because the counter anions affect the degree of solvation of the water molecules. This study is the first demonstration showing that the redox behaviour of cationic π-conjugated compounds changes upon applying hydrostatic pressure.

Results and discussion

Initial considerations

The cyclophane structure of dication $\mathbf{2}^{2+}$ is an ideal platform to study how pressure affects the redox behaviour of a cationic π-conjugated compound as the reversible two-stage 1e reduction that gives an isolable neutral biradical state $\mathbf{2}^{2\bullet}$ *via* radical cation state $\mathbf{2}^{\bullet+}$ can be examined (Fig. 1). In addition, despite the presence of only one kind of cationic chromophore, $\mathbf{2}^{\bullet+}$ and $\mathbf{2}^{2+}$ are distinguishable based on their UV-Vis spectra. Although $\mathbf{2}^{\bullet+}$ could not be isolated, the spectral features and the molar extinction coefficients of the $\mathbf{2}^{\bullet+}$ salts were revealed using UV-Vis spectroscopy of an equimolar mixed solution of $\mathbf{2}^{2+}$ and $\mathbf{2}^{2\bullet}$ (Fig. S8, ESI†). 4-Methoxyphenyl and 5-(4-methoxyphenyl)-thienyl groups were selected as the aryl groups at the 9-position of the xanthylium unit to investigate the influence that the

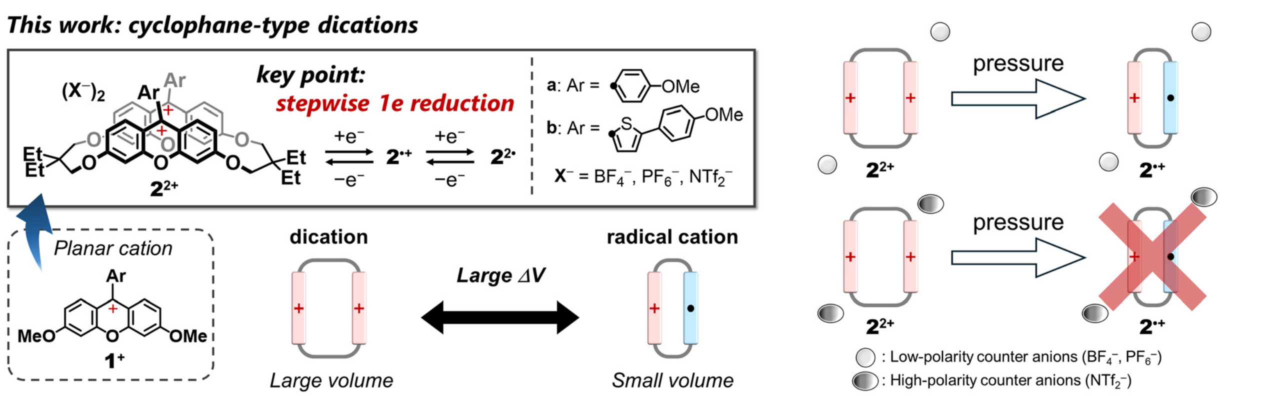

Fig. 1 Schematic illustration of the system reported in this work.

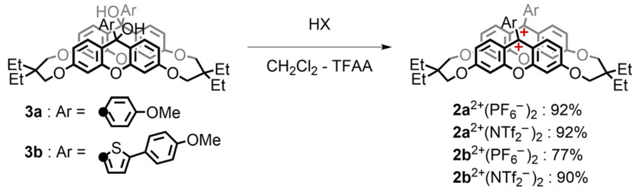

Scheme 1 Preparation of $\mathbf{2}^{2+}(PF_6^-)_2$ and $\mathbf{2}^{2+}(NTf_2^-)_2$.

conjugation of the π system has on the redox behaviour. We selected three anions, *i.e.*, BF_4^-, PF_6^-, and NTf_2^-, as the counterions to gain insights into the effect that their polarisation has on the redox behaviour. As shown in Scheme 1, the salts of $\mathbf{2}^{2+}(PF_6^-)_2$ and $\mathbf{2}^{2+}(NTf_2^-)_2$ were newly prepared from the corresponding diols using a procedure similar to the formation of $\mathbf{2}^{2+}(BF_4^-)_2$.[41]

Pressure-dependent UV-Vis spectra

Before investigating how the application of pressure affects the UV-Vis spectra for $\mathbf{2}^{2+}$, the counterion dependency of the UV-Vis spectra for $\mathbf{2}^{2+}$ under atmospheric pressure conditions was examined. For that purpose, the UV-Vis spectra of the BF_4^-, PF_6^-, and NTf_2^- salts of $\mathbf{2}^{2+}$ were measured in dehydrated CH_2Cl_2 (c = 0.81–1.75 × 10^{-5} M; Fig. S7, ESI†). All macrocyclic dications exhibit strong absorptions in the visible region which correspond to the two xanthylium chromophores [λ_{max}/nm (log ε): 420 (5.00) for $\mathbf{2a}^{2+}(BF_4^-)_2$, 422 (4.93) for $\mathbf{2a}^{2+}(PF_6^-)_2$, 425 (5.05) for $\mathbf{2a}^{2+}(NTf_2^-)_2$, 434 (4.79) for $\mathbf{2b}^{2+}(BF_4^-)_2$, 435 (4.86) for $\mathbf{2b}^{2+}(PF_6^-)_2$, and 437 (4.93) for $\mathbf{2b}^{2+}(NTf_2^-)_2$]. There is almost no difference in the λ_{max} and log ε values of $\mathbf{2}^{2+}(BF_4^-)_2$, $\mathbf{2}^{2+}(PF_6^-)_2$, and $\mathbf{2}^{2+}(NTf_2^-)_2$, which means that the UV-Vis spectra of $\mathbf{2}^{2+}$ do not depend on the counter anions, and thus, under these highly dilute conditions, ion pairing between the cyclophane dication and counter anion can be expected to be negligible.

Subsequently, to investigate the response of $\mathbf{2}^{2+}$ to hydrostatic pressure, the UV-Vis spectra of $\mathbf{2}^{2+}(BF_4^-)_2$ were measured under various hydrostatic pressures. Here, $\mathbf{2}^{2+}$ is expected to exhibit a response to hydrostatic pressure when the value of ΔV_T° is negative and it is known that the value of ΔV_T° depends on the solvent. Upon measuring the pressure-dependent UV-Vis spectra of $\mathbf{2}^{2+}(BF_4^-)_2$ in dehydrated and water-containing solvents, we found that $\mathbf{2}^{2+}(BF_4^-)_2$ exhibits unique behaviour in water-containing solvents. In the case of $\mathbf{2a}^{2+}(BF_4^-)_2$ in CH_2Cl_2/H_2O (v/v = 2000/3; c = 2.90 × 10^{-5} M; 2870 equiv. of H_2O molecules per molecule of $\mathbf{2a}^{2+}$), the UV-Vis spectrum of $\mathbf{2a}^{2+}(BF_4^-)_2$ continuously changed with increasing pressure and a decrease in the absorption band at ∼420 nm was observed. Meanwhile, a new peak appeared at ∼450 nm, which was assigned to the absorption of $\mathbf{2a}^{\bullet+}BF_4^-$ (Fig. 2a). It is likely that a minute amount of hydroxide ions in the solution acts as a reductant.[42] Similar pressure-dependent behaviour was observed for $\mathbf{2b}^{2+}(BF_4^-)_2$ in CH_2Cl_2/H_2O (v/v = 2000/3; c = 1.71 x 10^{-5} M; 4870 equiv. of H_2O molecules per molecule of $\mathbf{2b}^{2+}$) (Fig. S9a, ESI†). Thus, the 1e reduction of $\mathbf{2}^{2+}(BF_4^-)_2$ leading to the formation of radical cationic species was observed in both cases. On the other hand, the UV-Vis spectra

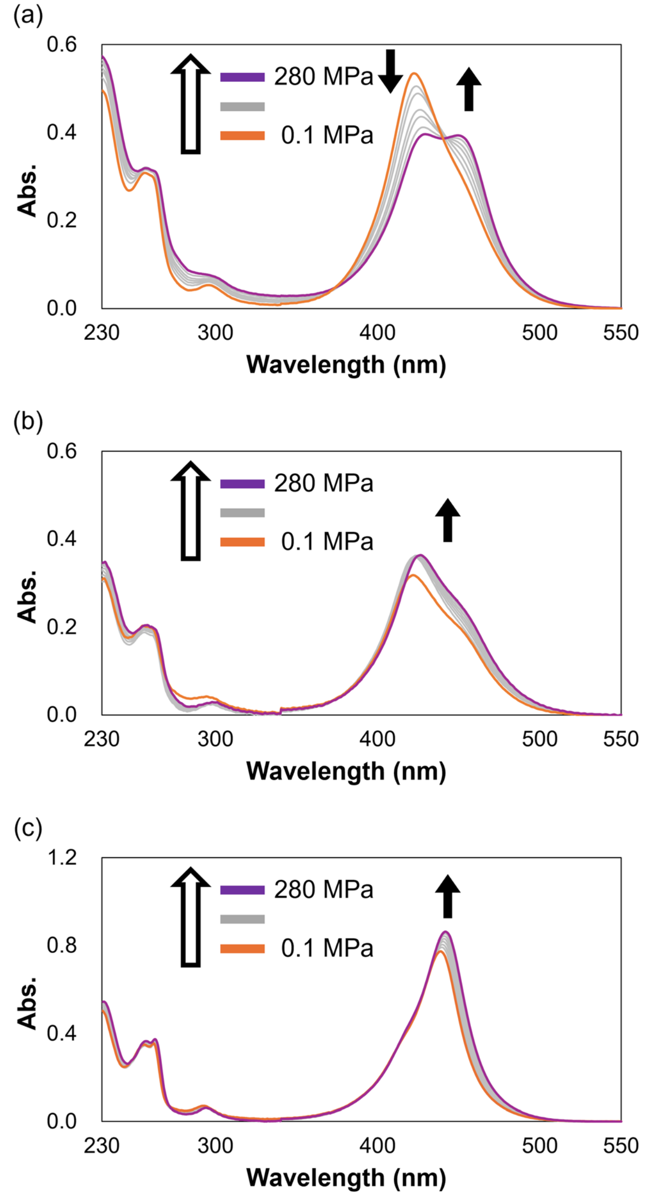

Fig. 2 Room-temperature pressure-dependent UV-Vis spectra of (a) $\mathbf{2a}^{2+}(BF_4^-)_2$ in CH_2Cl_2/H_2O (v/v = 2000/3; c = 2.90 × 10^{-5} M), (b) $\mathbf{2a}^{2+}(BF_4^-)_2$ in dehydrated CH_2Cl_2 (c = 2.82 × 10^{-5} M), and (c) $\mathbf{1a}^{+}BF_4^-$ in CH_2Cl_2/H_2O (v/v = 100/1; c = 4.65 × 10^{-5} M) at 0.1, 40, 80, 120, 160, 200, 240, and 280 MPa, measured in a high-pressure cell (path length: 2 mm; response: medium; scan rate: 100 nm min^{-1}).

of $\mathbf{2}^{2+}(BF_4^-)_2$ in dehydrated CH_2Cl_2 were remarkedly different. Here, a gradual increase of the absorbance at ∼430 nm was observed upon applying hydrostatic pressure, and only a slight red shift was observed without any significant changes in the spectral shape (Fig. 2b and Fig. S9b, ESI†). This behaviour is typical for π-conjugated compounds,[5,7] indicating that $\mathbf{2}^{2+}(BF_4^-)_2$ maintains its dicationic state upon being subjected to hydrostatic pressurisation in dehydrated solvents. Moreover, the monotonic hyperchromic effect observed only occurred because of the compression of the solution upon hydrostatic pressurisation. These results suggest that the presence of a small amount of water is essential for the observed 1e reduction of $2^{2+}(BF_4^-)_2$ upon hydrostatic pressurisation. It should also be noted here that when the pressure-dependent UV-Vis spectrum of monocation $\mathbf{1a}^+BF_4^-$ was measured in CH_2Cl_2/H_2O (v/v = 100/1; $c = 4.65 \times 10^{-5}$ M; 12 800 equiv. of H_2O per molecule of $\mathbf{1a}^+$) (Fig. 2c), only a gradual increase in the absorbance and a red shift were observed, as is the case for $2^{2+}(BF_4^-)_2$ in dehydrated CH_2Cl_2, indicating that $1^+BF_4^-$ maintains its cationic state upon hydrostatic pressurisation, even in water-containing solvents. Therefore, the cyclophane structure is essential for 1e reduction and the generation of the radical cationic state of $2^{2+}(BF_4^-)_2$ under exposure to hydrostatic pressure in water-containing solvents. The reversibility of redox reactions was confirmed by the one-electron oxidation of as-generated radical cationic species (Fig. S11, ESI†).

Reaction-volume changes

To investigate the response of 2^{2+} to hydrostatic pressure in detail, we calculated ΔV_T° according to eqn (5), where K is the abundance ratio of $2^{\bullet+}/2^{2+}$ for the 1e reduction.

$$\left(\frac{\partial \ln K}{\partial P}\right)_T = -\frac{\Delta V_T^\circ}{RT} \tag{5}$$

The values of K were assumed to be the concentration ratio of $2^{\bullet+}/2^{2+}$. We calculated the values of K using a simultaneous equation for the absorbance at λ_{max} of radical cation $2^{\bullet+}$ and dication 2^{2+}. As shown in Fig. 3, the natural logarithm of the value of the ratio of $\mathbf{2a}^{\bullet+}/\mathbf{2a}^{2+}$ was plotted as a function of the pressure, which furnished a good linear correlation. The line fitted to this data showed an excellent linear relationship [$r = 0.977$ for $\mathbf{2a}^{\bullet+}BF_4^-/\mathbf{2a}^{2+}(BF_4^-)_2$; the value of ln K at 280 MPa was excluded because it was almost saturated]. The values of ΔV_T° obtained from the slope of the plot were relatively large negative values [$\Delta V_T^\circ = -25.4 \pm 2.8\ cm^3\ mol^{-1}$ for $\mathbf{2a}^{2+}(BF_4^-)_2$], indicating not only that the desolvation of H_2O molecules occurs due to the decrease of cationic moieties caused by redox reaction, but also that a conformational change caused by the reduction of the electrostatic repulsion between the xanthylium units of the cyclophane-type dications occurred.

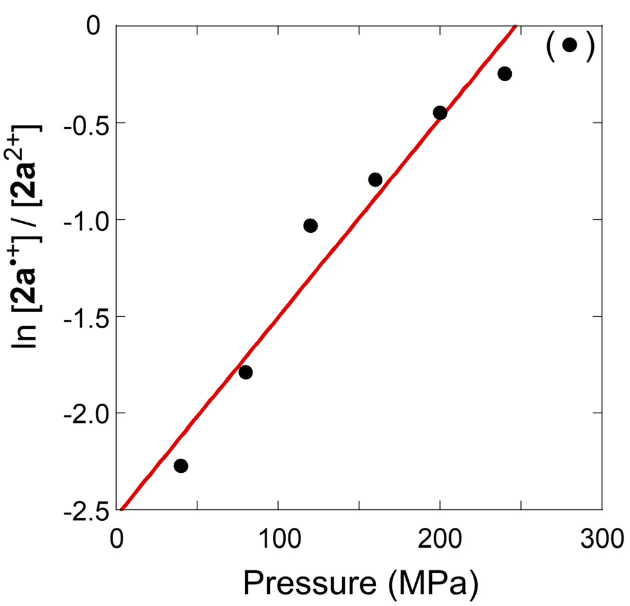

Fig. 3 Pressure dependency of the concentration ratio ($\mathbf{2a}^{2+}/\mathbf{2a}^{\bullet+}$) in CH_2Cl_2/H_2O (v/v = 2000/3) at room temperature (correlation coefficient $r = 0.977$).

Theoretical studies

To gain insight into the conformational changes of the cyclophane-type dication 2^{2+} and radical cation $2^{\bullet+}$, the intramolecular $\pi\cdots\pi$ contacts were investigated using density functional theory (DFT) calculations at the (U)ωB97X-D/6-31G* level. Identical values were obtained when calculated under pressure conditions of 280 MPa (Fig. S13–S16, ESI† and Table 1). As shown in Fig. 4, the shortest C···C distance between the π units for the radical cations is 0.07–0.08 Å shorter than for the dications (3.25 Å for $\mathbf{2a}^{2+}$; 3.17 Å for $\mathbf{2a}^{\bullet+}$; 3.24 Å for $\mathbf{2b}^{2+}$; 3.17 Å for $\mathbf{2b}^{\bullet+}$), suggesting that $2^{\bullet+}$ has a smaller van der Waals volume than 2^{2+}. This result indicates that the electrostatic repulsion between the cationic π units of 2^{2+} decreased upon injection of an electron into 2^{2+}. In addition, to investigate the

Table 1 The shortest C···C distance between the π units of $\mathbf{2a}^{2+}$, $\mathbf{2a}^{\bullet+}$, $\mathbf{2b}^{2+}$, and $\mathbf{2b}^{\bullet+}$ obtained using DFT calculations at the (U)ωB97X-D/6-31G* level at 280 MPa without and with the use of the self-consistent reaction field (SCRF) method

	The shortest C···C distance between cation units (Å) using the SCRF method (solvent)	
$\mathbf{2a}^{2+}$	None	3.25
	CH_2Cl_2	3.27
	H_2O	3.27
$\mathbf{2a}^{\bullet+}$	None	3.17
	CH_2Cl_2	3.20
	H_2O	3.21
$\mathbf{2b}^{2+}$	None	3.24
	CH_2Cl_2	3.23
	H_2O	3.24
$\mathbf{2b}^{\bullet+}$	None	3.17
	CH_2Cl_2	3.19
	H_2O	3.20

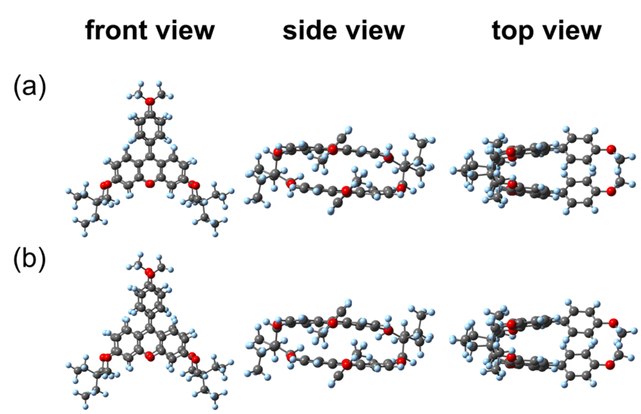

Fig. 4 Optimised structures for (a) $\mathbf{2a}^{2+}$ and (b) $\mathbf{2a}^{\bullet+}$ obtained from DFT calculations at the (U)ωB97X-D/6-31G* level at 280 MPa.

effect of solvation on the π···π distance in 2^{2+} and $2^{\bullet+}$, we also conducted DFT calculations at the (U)ωB97X-D/6-31G* level using the self-consistent reaction field (SCRF) method[43] (Fig. S13–S16, ESI†). With regard to the polarity, regardless of the solvent, the calculated C···C distance between the π units of 2^{2+} remained almost unchanged. A similar trend was observed for $2^{\bullet+}$. Since the bulk solvent effect on the distance between the π units was negligible in both 2^{2+} and $2^{\bullet+}$, the difference in the intramolecular π···π contacts can be inferred from the number of positive charges on the molecular unit. Thus, the value of ΔV_T° when going from the dication to the radical cation can be attributed to desolvation and a decrease in electrostatic repulsion.

Pressure-dependent UV-Vis spectra of 2^{2+} with different counter anions

Next, to investigate the effect that the counter anion has on the redox behaviour of the dications, pressure-dependent UV-Vis spectra of $2^{2+}(PF_6^-)_2$ and $2^{2+}(NTf_2^-)_2$ were measured in dehydrated CH_2Cl_2 and CH_2Cl_2/H_2O (v/v = 2000/3) (Fig. 5). Upon hydrostatic pressurisation in dehydrated CH_2Cl_2, gradual increases in the absorbance at ∼420 nm and a red shift were observed for both **2a**$^{2+}(PF_6^-)_2$ and **2a**$^{2+}(NTf_2^-)_2$ similar to those seen in **2a**$^{2+}(BF_4^-)_2$, which is typical behaviour for normal π-conjugated molecules. Upon hydrostatic pressurisation in CH_2Cl_2/H_2O (v/v = 2000/3), the UV-Vis spectrum of **2a**$^{2+}(PF_6^-)_2$ changed, *i.e.*, the absorption band at ∼420 nm decreased and a new peak emerged at ∼450 nm derived from the generation of **2a**$^{\bullet+}PF_6^-$. This finding indicates that a radical cation was formed $\left(\Delta V_T^{\circ} = 3.2 \pm 0.5\,\mathrm{cm^3\,mol^{-1}}\right)$ similar to the case of the BF_4^- salt. Conversely, **2a**$^{2+}(NTf_2^-)_2$ exhibited typical behaviour for a π-conjugated compound under pressure, even in CH_2Cl_2/H_2O (v/v = 2000/3). These results indicate that the redox behaviour of **2a**$^{2+}$ under hydrostatic pressure was clearly affected by the counter anion. Similar anion-dependent behaviour was observed in **2b**$^{2+}(PF_6^-)_2$ and **2b**$^{2+}(NTf_2^-)_2$ using pressure-dependent UV-Vis spectroscopy (Fig. S9, ESI†).

Thus, in addition to the cyclophane-type structure, the involvement of H_2O molecules in the solvation is crucial for the observed unique behaviour. In the case of the less polar anions BF_4^- and PF_6^-, both of which are less solvated by H_2O than the dication, the H_2O molecules preferentially solvate the cyclophane-type dication 2^{2+} to facilitate the reduction (Fig. 6a). Meanwhile, in the case of the more strongly polar NTf_2^- anion, the reduction does not proceed for $2^{2+}(NTf_2^-)_2$ even in a water-containing solvent (Fig. 6b), as the H_2O molecules would preferentially solvate the counter anions rather than the cyclophane-type dication 2^{2+}, which indicates that high hydrostatic pressurisation itself does not cause the 1e reduction of 2^{2+}. The desolvation of the H_2O molecules from the H_2O-solvated cyclophane-type dications occurs upon hydrostatic pressurisation in water-containing solvents. As a result, this desolvation process can trigger the 1e reduction of $2^{2+}(BF_4^-)_2$ and $2^{2+}(PF_6^-)_2$ because their ΔV_T° terms can be expected to be negative due to the cyclophane structure. This study suggests that the solvation of H_2O molecules is involved in the 1e

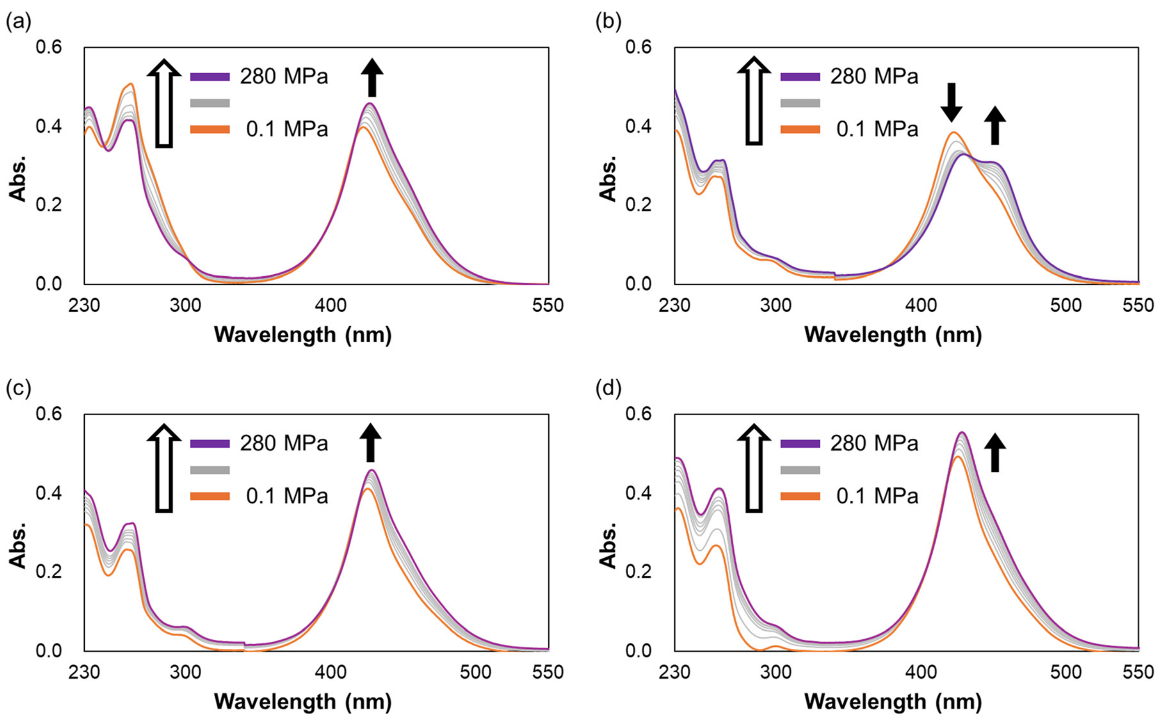

Fig. 5 Room-temperature pressure-dependent UV-Vis spectra of (a) **2a**$^{2+}(PF_6^-)_2$ in dehydrated CH_2Cl_2 (c = 2.36 × 10^{-5} M), (b) **2a**$^{2+}(PF_6^-)_2$ in CH_2Cl_2/H_2O (v/v = 2000/3; c = 2.29 × 10^{-5} M; 3630 equiv. of H_2O molecules are contained per **2a**$^{2+}$), (c) **2a**$^{2+}(NTf_2^-)_2$ in dehydrated CH_2Cl_2 (c = 1.82 × 10^{-5} M), and (d) **2a**$^{2+}(NTf_2^-)_2$ in CH_2Cl_2/H_2O (v/v = 2000/3; c = 2.18 x 10^{-5} M; 3820 equiv. of H_2O molecules are contained per **2a**$^{2+}$) at 0.1, 40, 80, 120, 160, 200, 240, and 280 MPa, measured in a high-pressure cell (path lengh: 2 mm; response: medium; scan rate: 100 nm min^{-1}).

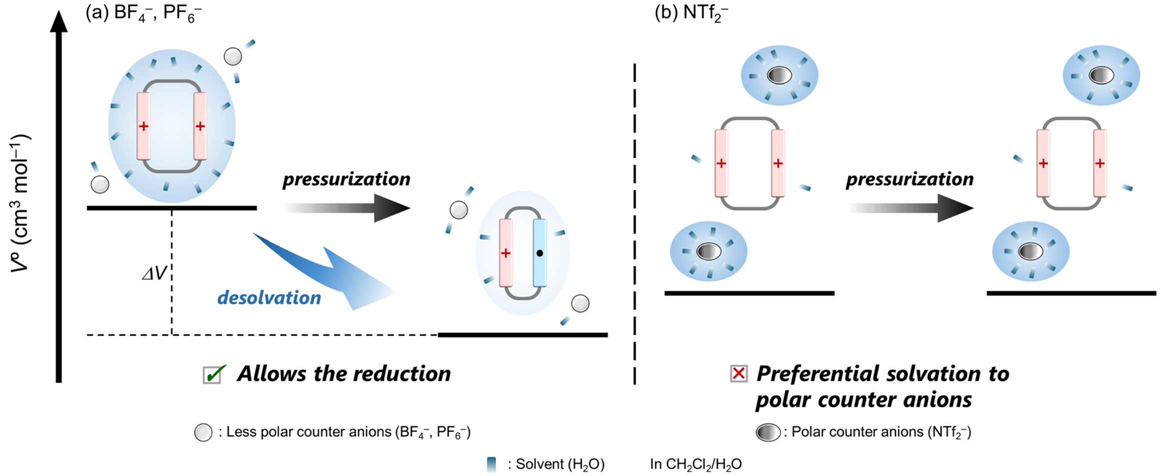

Fig. 6 Schematic illustration of (a) the volumetric changes during the reduction of $\mathbf{2}^{2+}(BF_4^-)_2$ and $\mathbf{2}^{2+}(PF_6^-)_2$ in CH_2Cl_2/H_2O (v/v = 2000/3) and (b) the preferential solvation of the counter anions of $\mathbf{2}^{2+}(NTf_2^-)_2$ in CH_2Cl_2/H_2O (v/v = 2000/3).

reduction under high hydrostatic pressure, and furthermore that the reduction of $\mathbf{2}^{2+}$ is also facilitated by the cyclophane structure.

Conclusions

The reduction of $\mathbf{2}^{2+}(BF_4^-)_2$ and $\mathbf{2}^{2+}(PF_6^-)_2$, *i.e.*, dications with a cyclophane structures, proceeded when hydrostatic pressure was applied in water-containing solvents. The key factor driving this reduction is the large negative value for the change in the apparent reaction volume at a certain constant temperature T (ΔV_T°). DFT calculations suggested that the large negative value of ΔV_T° is due to desolvation of the H_2O molecules and the change in the proximity between the π units caused by a 1e reduction accompanied by a decrease in electrostatic repulsion. Indeed, monocation $\mathbf{1}^{+}BF_4^-$ did not undergo a 1e reduction upon hydrostatic pressurisation, even in water-containing solvents, indicating that the redox behaviour is made possible by the cyclophane structure. In addition, $\mathbf{2}^{2+}(NTf_2^-)_2$ did not exhibit the reduction behaviour, even when hydrostatic pressure was applied in water-containing solvents, indicating that the reduction behaviour can be adjusted and controlled *via* judicious selection of the counter anion. Therefore, this study provides valuable guidelines for the rational design of molecules with redox behaviour that can be modulated using hydrostatic pressure, whilst it opens the doors to the development of novel pressure- and redox-responsive molecules.

Author contributions

Y. I. developed the concept of this study. M. K. conducted the synthetic and spectroscopic experiments as well as the theoretical calculations. T. K. and G. F. contributed to the spectroscopic studies under hydrostatic pressure. Y. I., G. F., and T. S. supervised the project. M. K., Y. I., and G. F. prepared the manuscript with feedback from all authors.

Conflicts of interest

There are no conflicts to declare.

Data availability

The data supporting this article have been uploaded as part of the ESI.†

Acknowledgements

This work was supported by Grant-in-Aid from MEXT and JSPS (No. JP25KJ0481 to M. K., JP23H04020, JP24K01536, and JP24K21791 to G. F., JP25K08604 to T. S., and JP23H04011, JP25H00873, and JP25H01259 to Y. I.) and JST PRESTO (JPMJPR23Q1 to Y. I). Y. I. is grateful for the Toyota Riken Scholar Program. This work was also supported by the Research Program of ''Five-star Alliance'' in ''NJRC Mater. & Dev.'' MEXT.

References

1 O. Vybornyi, S. Liu and R. Häner, Stimuli-Responsive Supramolecular Polymers from Amphiphilic Phosphodiester-Linked Azobenzene Trimers, *Angew. Chem., Int. Ed.*, 2021, **60**, 25872–25877.
2 C. Stefaniu, M. Chanana, D. Wang, G. Brezesinski and H. Möhwald, Stimuli-Responsive Magnetite Nanoparticle Monolayers, *J. Phys. Chem. C*, 2011, **115**, 5478–5484.
3 K. Isayama, N. Aizawa, J. Y. Kim and T. Yasuda, Modulating Photo- and Electroluminescence in a Stimuli-Responsive π-Conjugated Donor–Acceptor Molecular System, *Angew. Chem. Int. Ed.*, 2018, **57**, 11982–11986.
4 B. Teichmann, M. Sárosi, K. Shoyama, M. A. Niyas, R. K. Dubey and F. Würthner, 'Invisible' Molecular Dynamics Revealed for a Conformationally Chiral π-Stacked Perylene Bisimide Foldamer, *Angew. Chem., Int. Ed.*, 2025, **64**, e202414069.

5 F. A. Bovey and S. S. Yanari, Effect of Solvent Polarizability on the Ultra-Violet Spectral Shifts of Aromatic Compounds, *Nature*, 1960, **186**, 1042–1044.
6 W. W. Robertson, Comparison of the Effects of High Pressure and Low Temperature on the Absorption Spectra of Some Condensed-Ring Aromatics, *J. Chem. Phys.*, 1960, **33**, 362–365.
7 H. Mizuno and G. Fukuhara, Solution-State Hydrostatic Pressure Chemistry: Application to Molecular, Supramolecular, Polymer, and Biological Systems, *Acc. Chem. Res.*, 2022, **55**, 1748–1762.
8 A. Drljaca, C. D. Hubbard, R. V. Eldik, T. Asani, M. V. Basilevsky and W. J. I. Noble, Activation and Reaction Volumes in Solution. 3, *Chem. Rev.*, 1998, **98**, 2167–2290.
9 J. Silva, A. C. Oliveira, T. C. R. G. Vieira, G. A. P. D. Oliveira, M. C. Suarez and D. Foguel, High-Pressure Chemical Biology and Biotechnology, *Chem. Rev.*, 2014, **114**, 7239–7267.
10 T. Asano, H. Furuta and H. Sumi, ''Two-Step'' Mechanism in Single-Step Isomerizations. Kinetics in Highly Viscous Liquid Phase, *J. Am. Chem. Soc.*, 1994, **116**, 5545–5550.
11 K. Nakasha and G. Fukuhara, Aggregation-Induced Emission-Based Polymer Materials: Ratiometric Fluorescence Responses Controlled by Hydrostatic Pressure, *ACS Appl. Polym. Mater.*, 2020, **2**, 2303–2310.
12 T. Kinoshita, Y. Haketa, H. Maeda and G. Fukuhara, Ground- and excited-state dynamic control of an anion receptor by hydrostatic pressure, *Chem. Sci.*, 2021, **12**, 6691–6698.
13 R. Ruloff, U. P. Seelbach, A. E. Merbach and F. Klärner, Molecular tweezers as synthetic receptors: the effect of pressure and temperature on the formation of host-guest complexes, *J. Chem. Phys.*, 2002, **15**, 189–196.
14 A. A. Hamdan, P. Bugnon, C. Saudan, P. G. Lye and A. E. Merbach, High-Pressure Studies as a Novel Approach in Determining Inclusion Mechanisms: Thermodynamics and Kinetics of the Host-Guest Interactions for α-Cyclodextrin Complexes, *J. Am. Chem. Soc.*, 2000, **122**, 592–602.
15 N. S. Isaacs, P. J. Nichols, C. L. Raston, C. A. Sandova and D. J. Young, Solution volume studies of a deep cavity inclusion complex of C_{60}: [p-benzylcalix[5]arene $\subset$ C_{60}], *Chem. Commun.*, 1997, 1839–1840.
16 Y. Takeda, H. Mizuno, Y. Okada, M. Okazaki, S. Minakata, T. Penfold and G. Fukuhara, Hydrostatic Pressure-Controlled Ratiometric Luminescence Responses of a Dibenzo[a,j]phenazine-Cored Mechanoluminophore, *ChemPhotoChem*, 2019, **3**, 1203–1211.
17 R. S. Phillips, E. W. Miles, G. Holtermann and R. S. Goody, Hydrostatic Pressure Affects the Conformational Equilibrium of Salmonella typhimurium Tryptophan Synthase, *Biochemistry*, 2005, **44**, 7921–7928.
18 J. M. Patel and R. S. Phillips, Effects of Hydrostatic Pressure on Stereospecificity of Secondary Alcohol Dehydrogenase from Thermoanaerobacter Ethanolicus Support the Role of Solvation in Enantiospecificity, *ACS Catal.*, 2014, **4**, 692–694.
19 G. Jenner, R. B. Salem, B. El'yanov and E. M. Gonikberg, Piezochemical Interpretation of (C···H···X) Hydrogen Transfer in Ene Reactions, *J. Chem. Soc., Perkin Trans. 2*, 1989, 1671–1675.
20 T. C. Huang, H. Y. Fu and C. T. Ho, Mechanistic Studies of Tetramethylpyrazine Formation under Weak Acidic Conditions and High Hydrostatic Pressure, *J. Agric. Food Chem.*, 1996, **44**, 240–246.
21 J. Motoori, T. Kinoshita, H. Chai, M. S. Li, S. M. Wang, W. Jiang and G. Fukuhara, Dynamic Control of Chiral Recognition in Water-Soluble Naphthotubes Induced by Hydrostatic Pressure, *ACS Nanosci. Au*, 2024, **4**, 435–442.
22 S. Ono, T. Kinoshita, H. Iwasaki, Y. Imai and G. Fukuhara, Ratiometric Chemosensors That Are Capable of Quantifying Hydrostatic Pressure Stimulus: A Case of Porphyrin Tweezers, *ACS Phys. Chem Au*, 2024, **4**, 510–521.
23 H. Kita, R. Yamakado, R. Fukuuchi, T. Konishi, K. Kamada, Y. Haketa and H. Maeda, Switching of Two-Photon Optical Properties by Anion Binding of Pyrrole-Based Boron Diketonates through Conformation Change, *Chem. – Eur. J.*, 2020, **26**, 3404–3410.
24 J. E. Leffler, The Enthalpy-Entropy Relationship And Its Implications For Organic Chemistry, *J. Org. Chem.*, 1955, **20**, 1202–1231.
25 M. Weh, K. Shoyama and F. Würthner, Preferential molecular recognition of heterochiral guests within a cyclophane receptor, *Nat. Commun.*, 2023, **14**, 243.
26 H. Chen, I. Roy, M. S. Myong, J. S. W. Seale, K. Cai, Y. Jiao, W. Liu, B. Song, L. Zhang, X. Zhao, Y. Feng, F. Liu, R. M. Young, M. R. Wasielewski and J. F. Stoddart, Triplet–Triplet Annihilation Upconversion in a Porphyrinic Molecular Container, *J. Am. Chem. Soc.*, 2023, **145**, 10061–10070.
27 S. T. Guo, P. F. Cui, X. R. Liu and G. X. Jin, Synthesis of Carborane-Backbone Metallacycles for Highly Selective Capture of n-Pentane, *J. Am. Chem. Soc.*, 2022, **144**, 22221–22228.
28 D. Hartmann, S. E. Penty, M. A. Zwijnenburg, R. Pal and T. A. Barendt, A Bis-Perylene Diimide Macrocycle Chiroptical Switch, *Angew. Chem., Int. Ed.*, 2025, **64**, e202501122.
29 N. Li, Y. Li, Z. Wang, T. Cao, C. Liu, H. Wang, G. Li and G. He, Directional Electron Flow in a Selenoviologen-Based Tetracationic Cyclophane for Enhanced Visible-Light-Driven Hydrogen Evolution, *Angew. Chem., Int. Ed.*, 2024, **63**, e202410525.
30 S. Garain, P. L. Li, K. Shoyama and F. Würthner, 2,3:6,7-Naphthalene Bis(dicarboximide) Cyclophane: A Photofunctional Host for Ambient Delayed Fluorescence in Solution, *Angew. Chem., Int. Ed.*, 2024, **63**, e202411102.
31 M. Weh, A. A. Kroeger, K. Shoyama, M. Grüne, A. Karton and F. Würthner, π–π Catalysis Made Asymmetric—Enantiomerization Catalysis Mediated by the Chiral π-System of a Perylene Bisimide Cyclophane, *Angew. Chem., Int. Ed.*, 2023, **62**, e202301301.
32 S. Garain, K. Shoyama, L. M. Ginder, M. Sárosi and F. Würthner, The Delayed Box: Biphenyl Bisimide Cyclophane, a Supramolecular Nano-environment for the Efficient Generation of Delayed Fluorescence, *J. Am. Chem. Soc.*, 2024, **146**, 22056–22063.

33 F. Xie, H. Mao, C. Lin, Y. Feng, J. F. Stoddart, R. M. Young and M. R. Wasielewski, Quantum Sensing of Electric Fields Using Spin-Correlated Radical Ion Pairs, *J. Am. Chem. Soc.*, 2023, **145**, 14922–14931.

34 B. Odell, M. V. Reddington, A. M. Z. Slawin, N. Spencer, J. F. Stoddart and D. J. Williams, Cyclobis(paraquat-p-phenylene). A Tetracationic Multipurpose Receptor, *Angew. Chem., Int. Ed. Engl.*, 1988, **27**, 1547–1550.

35 W. Geuder, S. Hünig and A. Suchy, Phanes with Two 4,4′-Bipyridinium Moieties—A New Class of Compounds, *Angew. Chem., Int. Ed. Engl.*, 1983, **22**, 489–490.

36 X. Y. Chen, H. Chen and J. F. Stoddart, The Story of the Little Blue Box: A Tribute to Siegfried Hünig, *Angew. Chem., Int. Ed.*, 2023, **62**, e202211387.

37 H. Han, Y. Huang, C. Tang, Y. Liu, M. D. Krzyaniak, B. Song, X. Li, G. Wu, Y. Wu, R. Zhang, Y. Jiao, X. Zhao, X. Y. Chen, H. Wu, C. L. Stern, Y. Ma, Y. Qiu, M. R. Wasielewski and J. F. Stoddart, Spin-Frustrated Trisradical Trication of PrismCage, *J. Am. Chem. Soc.*, 2023, **145**, 18402–18413.

38 L. Ren, Y. Han, L. Jiao, Y. Zou and J. Wu, Highly Strained, Fully π-Conjugated Porphyrin Cyclophanes: Template-free Synthesis and Global Aromaticity, *Angew. Chem., Int. Ed.*, 2025, **64**, e202418532.

39 Y. Shi, C. Li, J. Di, Y. Xue, Y. Jia, J. Duan, X. Hu, Y. Tian, Y. Li, C. Sun, N. Zhang, Y. Xiong, T. Jin and P. Chen, Polycationic Open-Shell Cyclophanes: Synthesis of Electron-Rich Chiral Macrocycles, and Redox-Dependent Electronic States, *Angew. Chem., Int. Ed.*, 2024, **63**, e202402800.

40 L. D. Gillès de Pélichy and E. T. Smith, Redox Properties of Mesophilic and Hyperthermophilic Rubredoxins as a Function of Pressure and Temperature, *Biochemistry*, 1999, **38**, 7874–7880.

41 M. Kikuchi, T. Tadokoro, T. Tachibana, S. Suzuki, T. Suzuki and Y. Ishigaki, Cation-Stacking Approach Enabling Interconversion between Bis(xanthylium) and its Reduced Species, *Chem. – Eur. J.*, 2024, **30**, e202401683.

42 J. K. Lee, D. Samanta, H. G. Nam and R. N. Zare, Micrometer-Sized Water Droplets Induce Spontaneous Reduction, *J. Am. Chem. Soc.*, 2019, **141**, 10585–10589.

43 J. Tomasi, B. Mennucci and R. Canni, Quantum Mechanical Continuum Solvation Models, *Chem. Rev.*, 2005, **105**, 2999–3094.

